Proceedings of the ASME 2013 Conference on Smart Materials, Adaptive Structures and Intelligent Systems
SMASIS2013
September 16-18, 2013, Snowbird, Utah, USA

SMASIS2013-3165

A VIBRATION ENERGY HARVESTING STRUCTURE, TUNABLE OVER A WIDE FREQUENCY RANGE USING MINIMAL ACTUATION

John Heit **David Christensen** **Shad Roundy**
Integrated Self-Powered Sensing Lab, Dept. of Mechanical Engineering, University of Utah, USA

ABSTRACT

This paper introduces a novel vibration energy harvesting structure with a resonance frequency that is tunable over a large range using a simple compact mechanical adjustment that alters the structural stiffness. The frequency tuning requires minimal actuation that can be "turned off" while maintaining the new resonance frequency. Testing shows that the natural frequency can be adjusted from 32 Hz to 85 Hz. The structure is coupled with an electromagnetic transducer to generate power. Test results at varying excitation frequencies and amplitudes demonstrate tunable power generation over a very wide bandwidth. In addition to frequency tunability, the structure is a nonlinear softening spring, which provides the added benefit of a passively wider bandwidth for specific ranges of the design parameters.

INTRODUCTION

There is a growing need in our highly technological world of smart structures and smart environments to know the states of complex systems. To gather this information an array of sensors nodes must be used. These network nodes have applications in manufacturing, robotics, medical and structural monitoring. For certain applications it is beneficial for these wireless nodes to use ambient energy such as solar, thermal gradients, or mechanical. Recently, harvesting ambient mechanical energy in the form of vibrations has been the center of much research [1-17]. The most common structure used is a linear resonant harvester. These structures have an intrinsic tradeoff between efficiency and bandwidth; namely, as the quality factor of the device is raised and mechanical damping lowered, the half power bandwidth becomes extremely narrow. This is problematic when the excitation frequency drifts or slight changes to the structure from environmental conditions or manufacturing tolerances cause alterations in its resonance frequency. To overcome this limitation several novel ideas have been presented. These include introducing multiple vibration modes [1], tuning the resonance frequency of the harvester to match the input frequency [2], and introducing nonlinearities into the system [3,6,12,13,14,17].

Many techniques and technologies have been implemented in order to control the fundamental frequency of resonant structures. Peters et. al. implemented a design with piezoelectric actuators that adjusts the spring stiffness by altering the geometry of the system. This method was able to adjust the resonance frequency from 66 to 89 Hz [2]. Work by Eichhorn et. al. and others have applied axial loads to cantilever beams in order to alter the frequency. Using this method Eichhorn et. al. was able to adjust the frequency from 150Hz to 215Hz [4,16,17]. A more complete overview detailing recent advancements in frequency tuning is presented in Table 1.

These different approaches each have their merits in different vibration environments. It stands to reason that for a fixed frequency harmonic input, a matched linear harvester will perform well. It has been shown through numerical simulation by Hoffman et. al. that for band-limited white noise and harmonic frequency sweeps a nonlinear mono-stable and bi-stable system will outperform an optimized linear system [5]. Futhermore, it has been shown that for pure Gaussian white noise, nonlinearity is not a determining factor in power generation [6]. Most vibration sources are neither single fixed frequency sources nor pure Gaussian white noise. In many real scenarios the characteristics of the input vibration frequency changes in time. Nonlinear structures can improve the robustness of harvesters in these situations [6]. However, active (or semi-active) tuning employed in conjunction with nonlinear structures has the potential to further expand the operation range of a vibration energy harvester.

In this paper a novel tunable energy harvesting structure is introduced. The structure is tunable over a wide frequency range using minimal actuation, and consumes no power to remain at the new resonant value. This device is suitable for vibration spectra that contain a single dominant frequency that drifts in a known region. The values of the tunable range as well as the actuation required for this device compare well with similar recent published work.

Reference	Author	Actuation Range	Low Frequency [Hz]	High Frequency [Hz]	Mean Frequency [Hz]	Tuning Range	Tuning Gain
[2]	Chistian Peters et. al.	10 V	66	89	78	±15%	2.3 Hz/V
[7]	Shyh-Chin Huang et. al.	35 mm	85.1	167	126	±32%	2.3 Hz/mm
[4]	C. Elchhorn et. al.	70 V	150	215	183	±18%	0.9 Hz/V
[8]	Ivo N. Ayala et. al.	2 mm	64	78	71	±10%	7.0 Hz/mm
[9]	Vinod R. Challa et. al.	N/A	22	32	27	±19%	N/A
[10]	Mohamed O. Mansour et. al.	54 mm	3.19	12	8	±58%	0.2 Hz/mm
	This Work	5 mm	32	85	58	±45%	10.4 Hz/mm

Table 1. Comparison of tunable energy harvester presented in this paper to recent comparable published works.

STRUCTURE DESCRIPTION AND FABRICATION

The complete structure as detailed in Fig. 1 is made up of three subsystems: the spring structure, the control structure, and the electromagnetic generator.

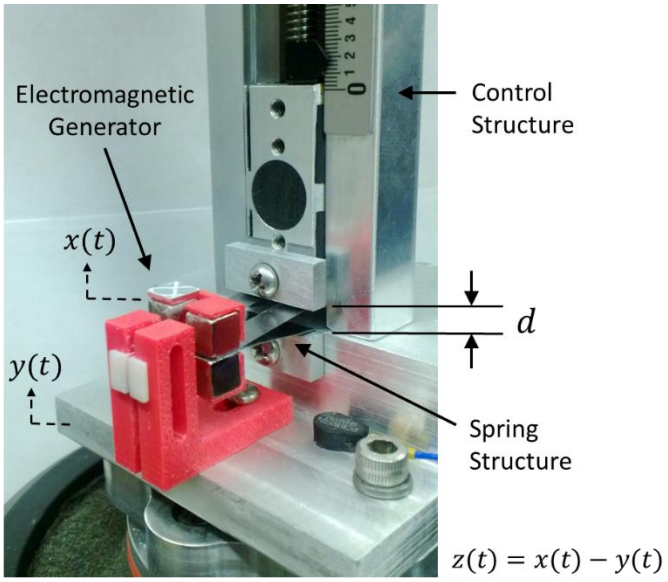

Figure 1. A photograph detailing the components of the system.

The innovation of this vibration energy harvester is the "wishbone" spring design shown in Fig. 2. The wishbone is constructed of two cantilever beams in parallel. The free ends of the beams are rigidly attached to each other and a proof mass. The fixed ends are clamped to the control structure. As the distance, d, between the beams increases, a component of the inertial force from the proof mass is transferred as an axial force through the spring. This effectively increases the stiffness of the spring structure as d is increased. In implementation two of these wishbone springs have been placed in parallel to accommodate the electromagnetic generator.

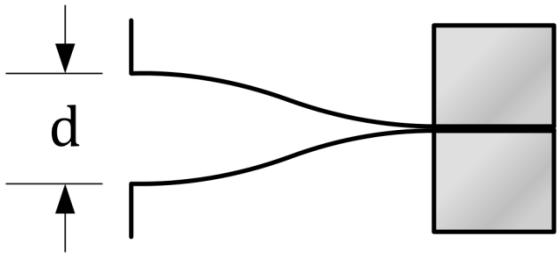

Figure 2. The wishbone spring configuration constructed of two cantilever beams in parallel.

The control structure tunes the resonance frequency of the spring structure by adjusting the separation distance d between the two beams. The test setup uses a dovetail slide to control d. This gives an adjustment resolution better than .0254mm (0.001").

The electromagnetic generator is used to transform the vibrational mechanical energy into electrical energy. The generator consists of a square coil between two sets of N52 Neodymium magnets. The electromagnetic generator is shown in Fig. 3. The springs were constructed using 0.004" thick low carbon steel. This was chosen to accommodate the tight bending radiuses required. Adhesive was used to connect the free end of the two beams to each other and the proof mass. The electromagnetic generator housing was constructed on a 3D printer. These generator parts consist of a spool of wire mounted on a bracket with the ability to be re-centered in the proof mass as d is varied.

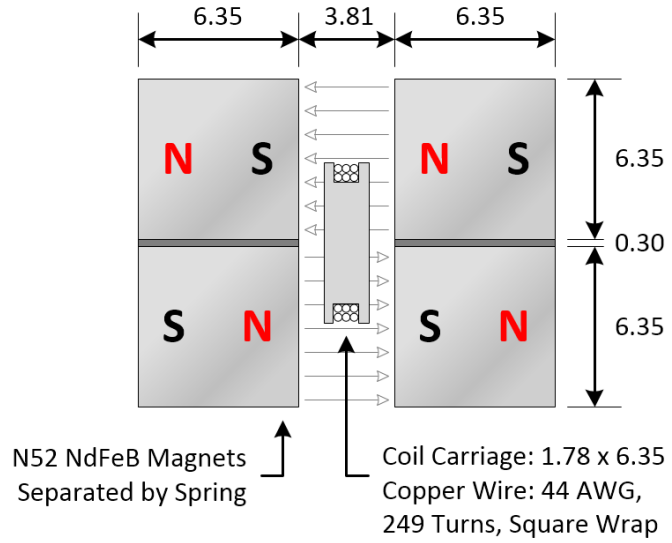

Figure 3. The proof mass is comprised of four 6.35mm cube N-52 Neodymium permanent magnets. The magnets are positioned such that the flux between the lower magnets is 180 degrees out of phase with the upper magnets. Dimensions are in mm.

THEORY AND MODELING

The system is modeled by the standard second order mass spring damper equation subjected to base excitation as in (1).

$$m\ddot{z}(t) + (c_e + c_m)\dot{z}(t) + k(d)z(t) = -m\ddot{y}(t) \quad (1)$$

Were m is the proof mass, c_e is the electrical damping coefficient from power generation, c_m is the mechanical viscous damping coefficient, and $k(d)$ is the spring constant of the wishbone spring structure, as function of d.

The equation as shown in (1) has the implicit assumption of a linear transducer whose electromagnetic force is directly proportional to the relative velocity of the proof mass, $\dot{z}(t)$. This assumes that the magnetic flux density between the top two magnets of the proof mass is uniform and that the magnetic flux density between the bottom two magnets is equal in magnitude and opposite in direction as shown in Fig. 3. The assumption holds with the caveat that the relative displacement of the proof mass, $z(t)$, must not exceed half the height of the generator coils. The electrical damping coefficient can then be calculated as in (2).

$$c_e = \frac{(2BhN)^2}{R} \quad (2)$$

Where B is the magnitude of the uniform magnetic flux density, h is the height of the square coil, N is the number of turns of the square coil, and R is the sum of the load resistance and coil resistance.

For a first order design of the electromagnetic generator, a mechanical damping ratio was estimated and the desired electrical damping ratio was set to match it. The coil plus load resistance was then calculated in terms of N and h as in (3), where ρ is the resistivity and A_w is the cross sectional area of the magnet wire. Substituting (3) into (2), the optimal N was then calculated as shown in (4).

$$R = 2N\rho\frac{(4h)}{A_w} \quad (3)$$

$$N = \frac{2c_e\rho(4h)}{(2Bh)^2A_w} \quad (4)$$

FEA simulations using FEMM yielded the flux through the square coil as a function of relative coil displacement, $z(t)$, and is shown in Fig. 5. Numerical results yield a maximum flux density of 0.6 T, which are in close agreement to the measured flux density of 0.58 T. The linear regression line fit of the flux plot demonstrates the limits of the linear transducer assumption described above. For this device, the expression $2Bh$ is equal to $0.006291\ Wb/m$ if the relative displacement of the proof mass does not exceed $\pm 2\ mm$.

The peak power generated from the linear transducer modeled in (1) is given in (5) [11], where ζ_e is the electrical damping ratio, ζ_t is the total damping ratio defined in (6), ζ_m is the mechanical damping ratio, A is the peak excitation acceleration, and r is the frequency ratio defined as $r = \omega/\omega_n$ with ω as the excitation frequency and ω_n as the natural frequency of the mass spring system. Equation (5) assumes that the generated power is equal to the power dissipated through the electrical damper. If the system is operating at resonance, (5) may be simplified as (7).

$$|P| = \frac{2m\zeta_e A^2 r^3}{(1-r^2)^2 + (2\zeta_t r)^2} \quad (5)$$

$$\zeta_t = \zeta_m + \zeta_e \quad (6)$$

$$|P| = \frac{m\zeta_e A^2}{2\omega\zeta_t^2} \quad (7)$$

From initial test data and characterization of the spring structure, $k(d)$ is known to be a mono-stable softening spring. The standard form for this spring type will be used and is shown in (8).

$$k(d) = k_5(d)x^5 + k_3(d)x^3 + k_1(d)x \quad (8)$$

Where $k_5(d)$ and $k_1(d)$ are positive coefficients and and $k_3(d)$ is a negative coefficient.

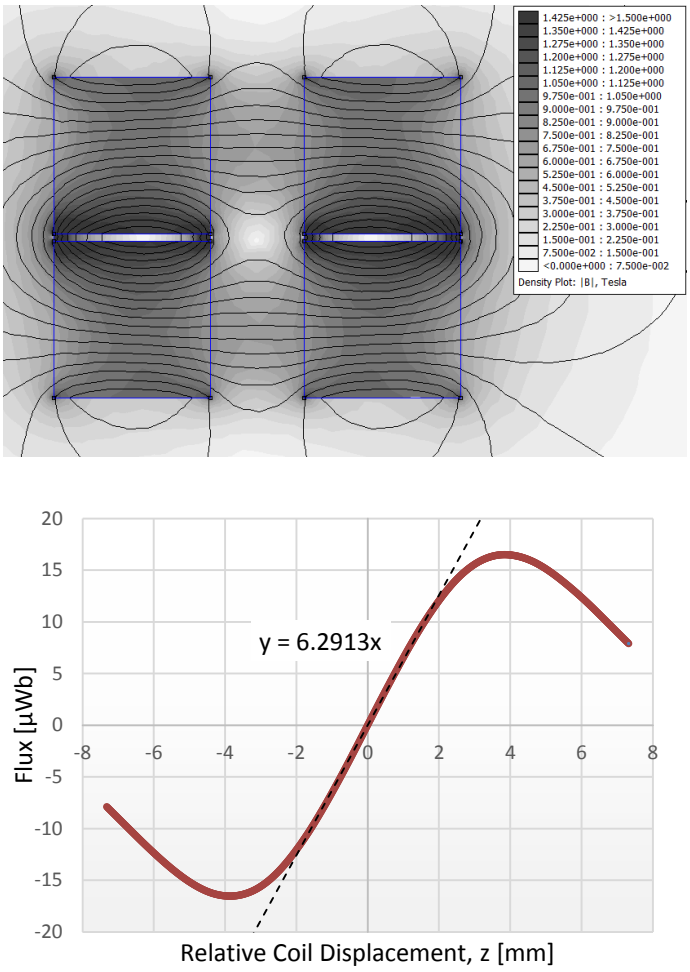

Figure 5. Top, FEM simulation of the flux density for the arrangement of the magnets. Numerical results of 0.6 T are in close agreement to the measured flux density of 0.58 T. Bottom, Flux through the area enclosed by the generator coils as a function of z. Notice that the system can be approximated as linear through a small displacement region of ~ ±2 mm.

EXPERIMENTAL METHODS

The system was empirically characterized to determine the stiffness of the spring structure as the distance d was adjusted. The force versus displacement as a function of the separation of the spring bases (d) was tested on an Instron. The data was collected for values of d ranging from 0 – 5mm (0 – 0.2") by 0.5mm (0.020") increments and is shown in Fig 6. During the testing the system was firmly secured and the load cell contacted at the center of the proof mass.

The dynamic response of the system was characterized by subjecting the device to a series of harmonic sweeps. These experiments were carried out using a Labworks shaker system. A laser vibrometer was used to measure the response of the proof mass. The system was controlled using Labview and closed loop feedback control to hold the peak acceleration constant through the entire frequency sweep.

The velocity signal from the laser vibrometer was differentiated and filtered to get the absolute acceleration of the proof mass. This acceleration signal was then divided by the signal from the accelerometer attached to the base of the system in order to get the system's dynamic response. Harmonic sweeps where performed from 20-100 Hz at various values of the base excitation and distances d. The acceleration values ranged from 0.2 – 0.5G at 0.1G intervals, and the base distance d ranged from 0 – 5mm (0 – 0.200") by 0.5mm (0.020") intervals. For large acceleration values the harmonic sweeps were not performed for small values of d due to physical constraints of the system. At the large acceleration values the displacement of the proof mass would be great enough to cause yielding of the spring material. Harmonic down sweeps at corresponding values of acceleration and d were also performed to demonstrate the nonlinearity of the spring structure.

The mechanical damping coefficient was empirically determined for the system. This was accomplished by giving the proof mass a set initial displacement and measuring the response with the laser vibrometer with no electrical load. This was done at 1mm (0.04") increments of d. This same test was carried out with two load resistances, 56 Ohms, the measured resistance of the coils, and 1000 Ohms. This data can then be used to determine the electrical damping of the system.

The voltage produced from the electromagnetic generator was recorded in order to verify the data from the laser vibrometer and to calculate the power generated. This voltage was measured across a resistor of equal value to the resistance of the coil windings.

RESULTS AND DISCUSSIONS

The results from the Instron testing show a dramatic increase in stiffness as d is increased. For large base separation (d) values, the stiffness becomes increasingly nonlinear. For large displacements the spring structure behaves as a softening spring. This effect is likely due to the lower, or inside beam, buckling as the tip is displaced downwards.

The Matlab™ curvefit toolbox was used to determine the coefficients of (8) as a function of d.

$$k_5(d) = 4.66e^{-3}d^2 - 3.51e^{-3}d \quad (13)$$
$$k_3(d) = -2.69e^{-3}d^2 - 2.32e^{-2}d \quad (14)$$
$$k_1(d) = -1.45e^{-2}d^3 + 0.14d^2 + 0.18e^{-3}d + 0.2685 \quad (15)$$

These equations show the global relationship of the of the spring structures stiffness as a function of d.

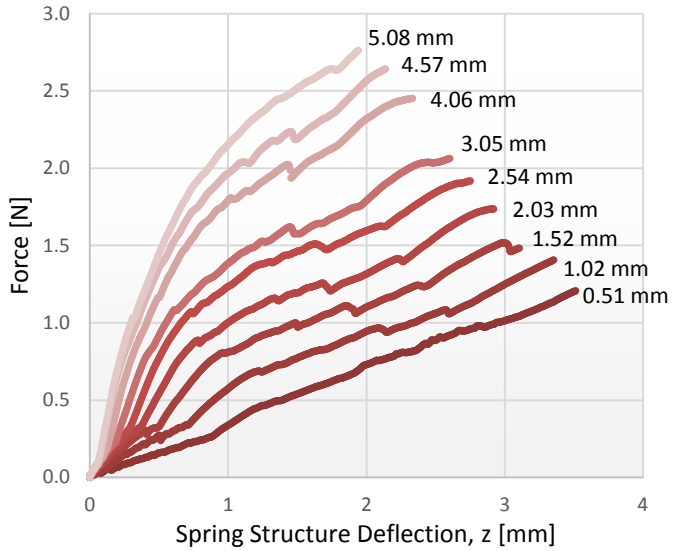

Figure 6. Results of the Instron testing. Used to obtain empirical force versus displacement plots of the spring structure for varying values of *d*.

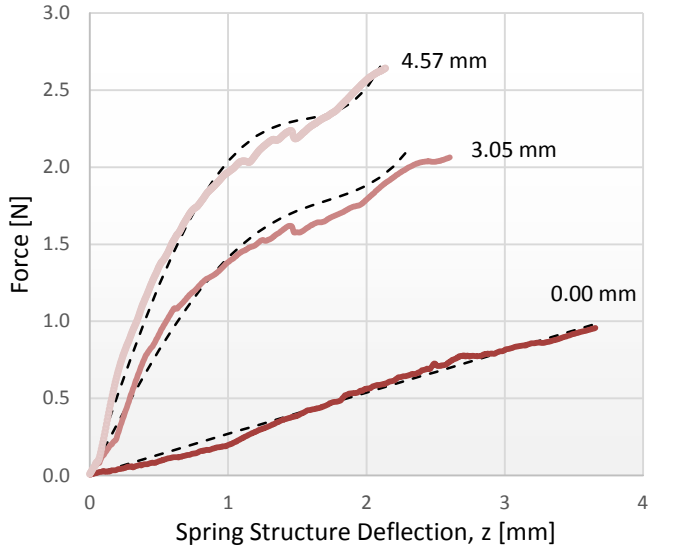

Figure 7. Curve fit models for select values of d.

For each harmonic frequency sweep the resonance frequency was recorded. For large acceleration values and separation distances *d*, where the spring structure behaves as a nonlinear softening spring, the frequency at which the peak voltage was recorded is used as the resonance frequency. Figure 8 shows the resonance frequency versus base separation (*d*) for all excitation acceleration values tested. Figure 9 shows the average resonance frequency for all the acceleration values.

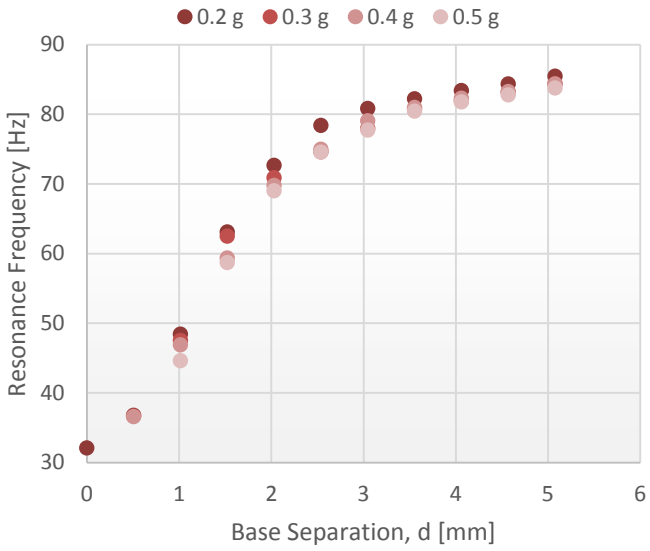

Figure 8. The resonance frequency for each tested value of base excitation acceleration, and separation of the spring bases d.

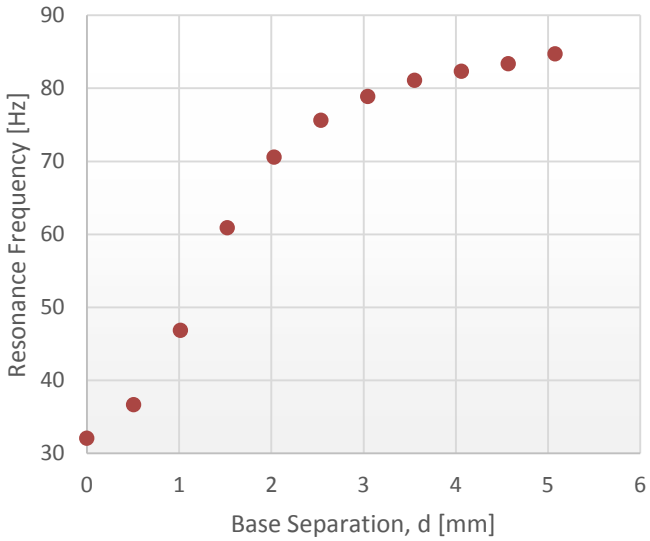

Figure 9. The Average resonance frequency of the system for all acceleration values as a function of the spring base separation.

The lowest average frequency, when the two beams are parallel is 32 Hz. With the bases of the springs displaced 5mm (0.200") the average resonance frequency increased to 85 Hz. This gives a median value for the resonance frequency of 59 Hz with a tuning range of ±45 percent. As is evident in Fig. 8 and Fig. 9, the system response changes much more drastically for lower values of *d*. For the first 2.5mm (0.100") of adjustment the system's resonance frequency increases by

approximately 140 percent from 32 Hz to 76 Hz. When the distance d is increased further, from 2.5mm (0.100") to 5mm (0.200") the system only increases an additional 28 percent; to 165 percent above the base frequency. The lower region of values of d is also where the system behaves as a linear spring.

For relatively large accelerations and base separations the spring structure behaves as a softening spring. Harmonic sweeps were run in both directions to demonstrate the dynamic response of the system. A prototypical response to these inputs is shown in Fig. 10. From the upward sweeps the response stays at the lower solution, and then suddenly jumps to the upper solution at high frequency. With the downward sweeps the response stays in the upper solution for a larger frequency range.

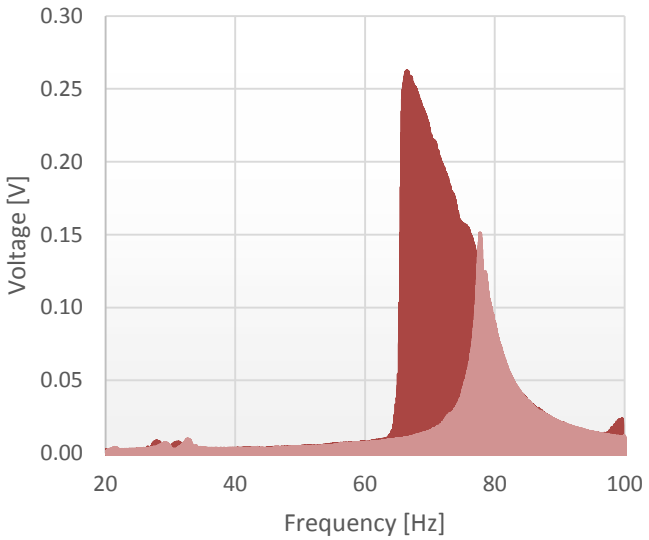

Figure 10. Harmonic sweeps from 20-100 Hz (light) and 100-20 Hz (dark) for accelerations of 500mG and a base separation of 3mm (0.120").

Figure 11 shows the resonance frequency versus base separation for two down sweeps. Compare this to the data in Fig. 8 for the up sweeps. For 0.2 G (the lower excitation value) the frequencies are nearly identical for up and down sweep. In other words, the system behaves linearly. However, for large excitation values, the resonance (or peak) frequency is different for the up and down sweeps indicating nonlinearity.

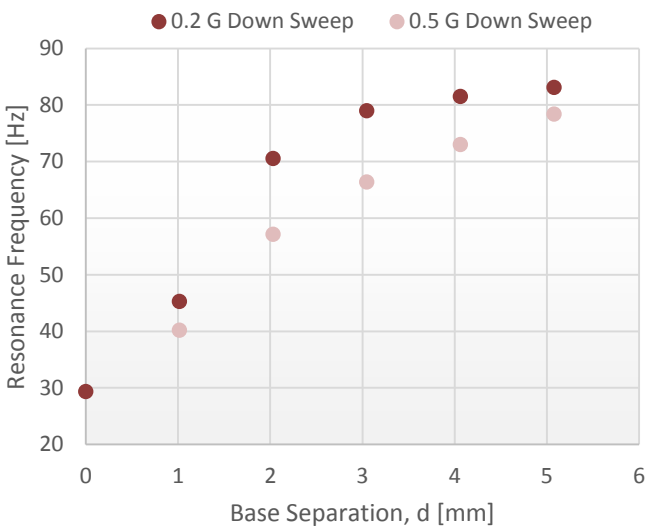

Figure 11. Resonance frequency response of the system to downward harmonic sweeps.

The mechanical quality factor, equal to $Q = 1/2\zeta_m$, was calculated from the response of the proof mass using the log decrement. It was found that for a zero value of d the quality factor of the system was quite low. This is due to the fact that at large displacement and low base separation the two beams contact each other. When the base separation was increased to a range of 1 - 3mm (.04" - .12") the quality factor rose to a near constant value. When d was further increased the quality factor greatly rose. The authors believe that this is due to a new vibration mode being introduced.

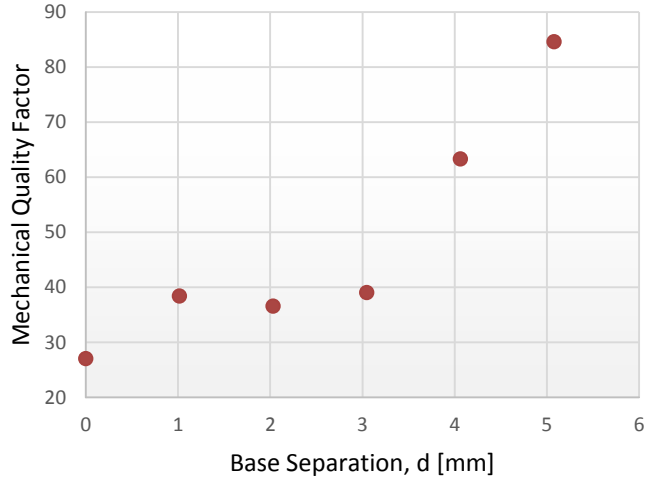

Figure 12. Mechanical quality factor of the system as a function of the base separation d.

By measuring the voltage across the load resistor the peak output power of the generator was calculated. This was done for each value of d. The peak power output at the 200mG level for the harmonic upsweeps was found to be 340 μW for a

base separation distance of zero. The power output slowly decreased until the mechanical quality factor rose to a level comparable to the quality factor of the electrical damping at high values of d. This general trend holds for all the upsweeps tested and is shown in Fig. 13.

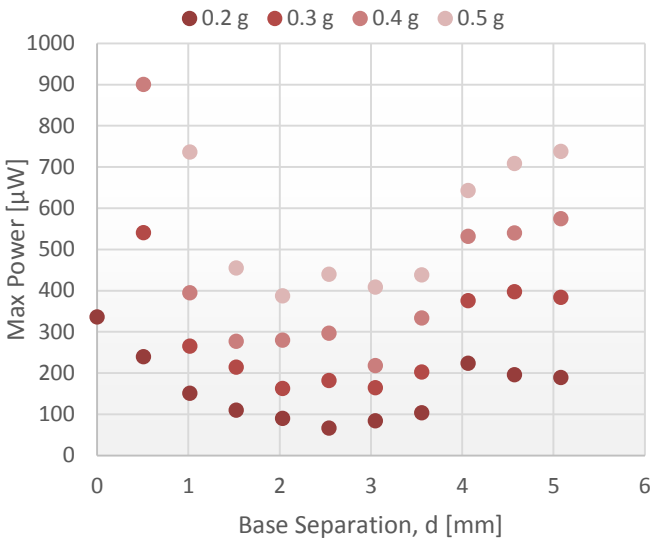

Figure 13. Peak power output of harmonic upsweeps for all tested values of base separation and acceleration.

For small input accelerations, the power versus base separation is similar for up sweeps and down sweeps as would be expected (see Fig. 14). However, for large acceleration values, the output power is much larger on the down sweep. This follows from the nonlinear softening behavior as shown in Fig. 10. Also, as is clear in Fig. 14, the output power is not a strong function of the base separation for larger input accelerations.

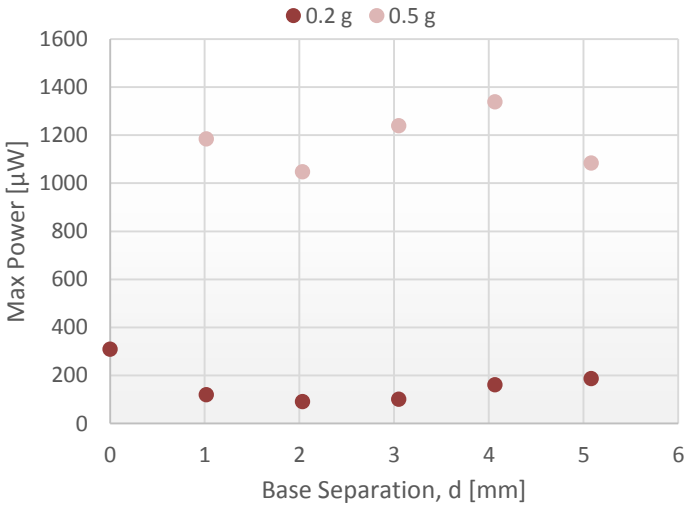

Figure 14. Max power output for harmonic down sweeps.

CONCLUSION AND FUTURE WORK

This paper has shown a tunable vibration energy harvester capable of adjusting the resonance frequency over a large range with minimal actuation. The spring structure of the device was characterized statically and dynamically using harmonic frequency sweeps. The results from both of these tests showed that the system behaves as a nonlinear softening spring for large separation values d and base excitations.

Further work should be carried out on characterizing the relationships between design parameters, such as length and thickness of the beam. This would allow for an optimization of parameters in the construction of a system built for harvesting energy from a known vibration spectrum.

An investigation into a low power consumption actuator to control the base separation d could also be made. This coupled with an optimal closed loop controller could lead to an energy efficient autonomous vibration energy harvester.

REFERENCES

[1] S. Roundy, "Improving Power Outpot for Vibration-Based Energ Scavengers," *IEEE Computer Society,* 2005.

[2] C. Peters, D. Maurath, W. Schock, F. Mezger and Y. Manoli, "A Closed-loop Wide-range Tunable Mechanical Resonator for Energy Harvesting Systems," *Journal of Micromechanics and Microengineering,* 2009.

[3] M. F. Daqaq, "On Intentional Introduction of Stiffness Nonlinearities for Energy Harvesting Under White Gaussian Excitations," *Nonlinear Dynamics,* vol. 69, no. 3, pp. 1063-1079, 2012.

[4] C. Eichhorn, R. Tchagsim, N. Wilhelm and P. Woias, "A Smart and Self-sefficient Frequency Tunable Vibration Energy Harvester," *Journal of Micromechanics and Microengineering,* 2011.

[5] D. Hoffmann, B. Folkmer and a. Y. Manoli, "Comparative Study of Concepts for Increasing the Bandwidth of Vibration Based Energy Harvesters," *PowerMEMs,* 2012.

[6] B. P. Mann, D. A. Barton and B. A. Owens, "Uncertainty in Performance for Linear and Nonlinear Energy Harvesting Strategies," *Journal of Intelligent Material Systems and Structures,* pp. 1451-1460, 2012.

[7] L. S.-C. Huang and Kao-An, "A Novel Design of a Map-tuning Piezoelectric Vibration Energy Harvester," *Smart Materials and Structures,* 2012.

[8] I. N. Ayala, D. Zhu, M. J. Tudor and S. P. Beeby, "Harvester, Autonomous Tunable Energy," *PowerMEMS,* 2009.

[9] V. R. Challa, M. G. Prasad, Y. Shi and F. T. Fisher, "A Vibration Energy Harvesting Device with Bidirectional Resonance Frequancy Tunability," *Smart Materials and Structures,* 2008.

[10] M. O. Mansour, M. H. Arafa and S. M. Megahed, "Resonator with Megnetically adjustable Natural

Frequency for Vibration Energy Harvesting," *Sensors and Actuators A: Physical,* 2010.

[11] C. Williams, C. Shearwood, M. Harradine, P. Mellor, T. Birch and R. Yates, "Development of an Electromagnetic Micro-generator," *IEE Proc. Circuits Devices Systems,* vol. 148, no. 6, 2001.

[12] S. C. Stanton, "Nonlinear Dynamcis for Broadband Energy Harvesting: Investigation of a bistable piezoelectric Inertial Generator," *Physica D,* 2010.

[13] A. Erturk and J. Hofmann, "A Piezomagnetoelastic Structure for Broadband Vibration Energy Harvesting".

[14] S. D. Nguyen and E. Halvorsen, "Bistable Springs for Wideband Microelectromechanical Energy Harvesters," *Applied Physics Letters,* 2012.

[15] F. Cottone, H. Vocca and L. Gammaitoni, "Nonlinear Energy Harvesting," *Physical REview Letters,* 2008.

[16] E. Leland and P. Wright, "Resonance Tuning of Piezoelectric Vibration Energy Scavenging Generators using Compressive Axial Preload," *IOP Science,* 2006.

[17] R. Masana and M. Daqaq, "Electromechanical Modeling and Nonlinear Analysis of Axially Loaded Energy Harvesters".